8. THE THERMAL BALANCE OF THE ATMOSPHERE OF VENUS

M. G. TOMASKO

Lunar and Planetary Laboratory, University of Arizona, Tucson, Ariz. 85721, U.S.A.

R.BOESE

Space Sciences Division, Ames Research Center, Moffett Field, Calif. 94035, U.S.A.

A. P. INGERSOLL

Division of Geological and Planetary Sciences, California Institute of Technology, Pasadena, Calif. 91125, U.S.A.

A. A. LACIS

Goddard Institute for Space Studies, National Aeronautics and Space Administration, New York, NY 10025, U.S.A.

S. S. LIMAYE

Space Science and Engineering Center, University of Wisconsin, Madison, Wis. 53703, U.S.A.

J. B. POLLACK

Space Sciences Division, Ames Research Center, Moffett Field Calif. 94035, U.S.A.

A. SEIFF

Space Sciences Division, Ames Research Center, Moffett Field, Calif. 94035, U.S.A.

A. I. STEWART

Laboratory for Atmospheric and Space Physics and Department of Astrogeophysics, University of Colorado, Boulder, Co. 80302, U.S.A.

V. E. SUOMI

Space Science and Engineering Center, University of Wisconsin, Madison, Wis. 53703, U.S.A.

and

F. W. TAYLOR

Jet Propulsion Laboratory, Pasadena, Calif. 91103, U.S.A.

Abstract. Current knowledge of the temperature structure of the atmosphere of Venus is briefly summarized. The principal features to be explained are the high surface temperature, the small horizontal temperature contrasts near the cloud tops in the presence of strong apparent motions, and the low value of the exospheric temperature. In order to understand the role of radiative and dynamical processes in maintaining the thermal balance of the atmosphere, a great deal of additional data on the global temperature structure, solar and thermal radiation fields, structure and optical properties of the clouds, and circulation of the atmosphere are needed. The ability of the Pioneer Venus Orbiter and Multiprobe Missions to provide these data is indicated.

Space Science Reviews **20** (1977) 389–412.

1. Introduction

Until about twenty years ago Venus was often described as 'Earth's Twin'. The diameter of Venus is only 4% less than that of the earth, and its mass is less than 20% smaller. Venus is about 28% closer to the sun than is the earth, but because of its reflective cloud cover, Venus absorbs somewhat less energy from the sun than the earth does. If the energy that Venus absorbs from the sun is balanced by 'black body' thermal re-radiation to space, the temperature of the 'radiation level' of the atmosphere of Venus should be about 240 K compared with 255 K for a similar calculation for the earth. Temperatures of about 250 K have been derived for a slightly lower level of Venus' atmosphere from the relative strengths of spectroscopic absorption lines involving the excitation of different rotational states of CO_2.

In 1956 however, strong microwave emission was detected from Venus. One explanation for this radiation was thermal emission from the surface of the planet. The required surface temperature was 600 K or greater – so surprisingly high that alternative non-thermal mechanisms for the microwave emission were sought. No satisfactory non-thermal mechanism could be found, however, and surface temperatures as high as 750 K subsequently have been measured directly by the Soviet Venera series of atmospheric entry probes.

The question of how a planet so similar to the Earth in other respects has developed a thick atmosphere and such a high surface temperature is an intellectually fascinating one. In addition, if the same processes that have led to the present thermal structure for the atmosphere of Venus can occur on earth, their understanding one day may assume a vital urgency for us.

The first step in understanding the evolution of planetary atmospheres must be to understand their current equilibrium. The present thermal balance of the atmosphere of Venus is unfortunately only poorly understood. Indeed, the temperature structure of the atmosphere is only partly known. In Section 2 we briefly summarize the current knowledge of the temperature structure of the Venusian atmosphere. The main features to be understood are the very high surface temperature, the form of the vertical temperature gradient, and the apparent small horizontal temperature gradients (both day–night and equator–pole) relative to earth despite an expected strong variation in the local deposition of solar energy over the illuminated hemisphere. In addition, the very low exospheric temperatures inferred from recent analyses of Mariner 5 and 10 airglow data must be explained.

Both radiative and dynamical transfer processes interact to determine the thermal balance of a planetary atmosphere. In Section 3 we discuss the role of radiative processes in the deposition of solar energy and its vertical redistribution. In particular, here we indicate the gaps in our knowledge which must be filled to evaluate the role of the greenhouse effect in sustaining the high surface temperature of Venus.

Should the greenhouse effect prove insufficient, dynamical effects may be required to understand the high surface temperature of Venus. In addition, dynamical heat transport will certainly be required to understand the global distribution of temperature over the planet. In Section 4 we identify some of the information which is needed before the dynamical redistribution of heat in the atmosphere of Venus can be understood.

In Section 5 we review in turn the key gaps in our knowledge of the planet's temperature structure and radiative and dynamical characteristics which need to be filled in order to understand the detailed local and global thermal balance of the atmosphere of Venus. For each of these areas, we indicate the extent to which the experiments aboard the Pioneer Venus missions can be expected to provide the required information.

2. Thermal Structure of the Atmosphere

In this section we briefly summarize the observations of the Venus atmospheric thermal structure. The lower atmosphere (from the surface to about 60 km altitude) has been measured by the Soviet entry probes, Veneras 4–10 (Marov, 1972; Marov *et al.*, 1973, 1976), and has been sounded from the earth using radars and microwave radiometers (cf., Rumsey *et al.*, 1974; Berge, Muhleman and Orton, 1972). The atmosphere from about 40 to 80 km altitude has been measured using the radio occultation technique applied to the U.S. spacecraft Mariners 5 and 10 (Fjeldbo, Kliore and Eshleman, 1971; Howard *et al.*, 1974). Infrared thermal emission from the cloud tops (at about 65 km altitude) has been observed from the earth (Murray, Wildey and Westphal, 1963; Westphal, Wildey and Murray, 1965) and from the Mariner 10 spacecraft (Chase *et al.*, 1974). Theoretical models (McElroy, 1968; Dickinson and Ridley, 1975) have been used to infer temperatures from above the cloud tops to the thermosphere. These temperatures can be compared with measurements of electron density scale heights inferred from radio occultation studies (Fjeldbo, Seidel and Sweetnam, 1975). The Regulus occultation in 1959 provided information about temperatures near the 115 to 120 km level (de Vaucouleurs and Menzel, 1960; Hunten and McElroy, 1968). Finally, Limb intensity profiles of hydrogen and helium airglow emissions observed by Mariner 5 and 10 yield the exospheric temperature (Anderson, 1976; Broadfoot *et al.*, 1974; Kumar and Broadfoot, 1975). Figure 1, from Marov (1972), shows a temperature profile from 0 to 130 km altitude.

2.1. Vertical thermal structure

One of the most basic scientific questions raised by these observations concerns the high surface temperature. The incident solar flux at Venus is about twice that at the earth, although the power absorbed is less than that at the earth because of Venus' relatively high albedo.Yet, for surface temperatures of Venus and the earth of 740 and 290 K respectively, the blackbody infrared flux emitted from the

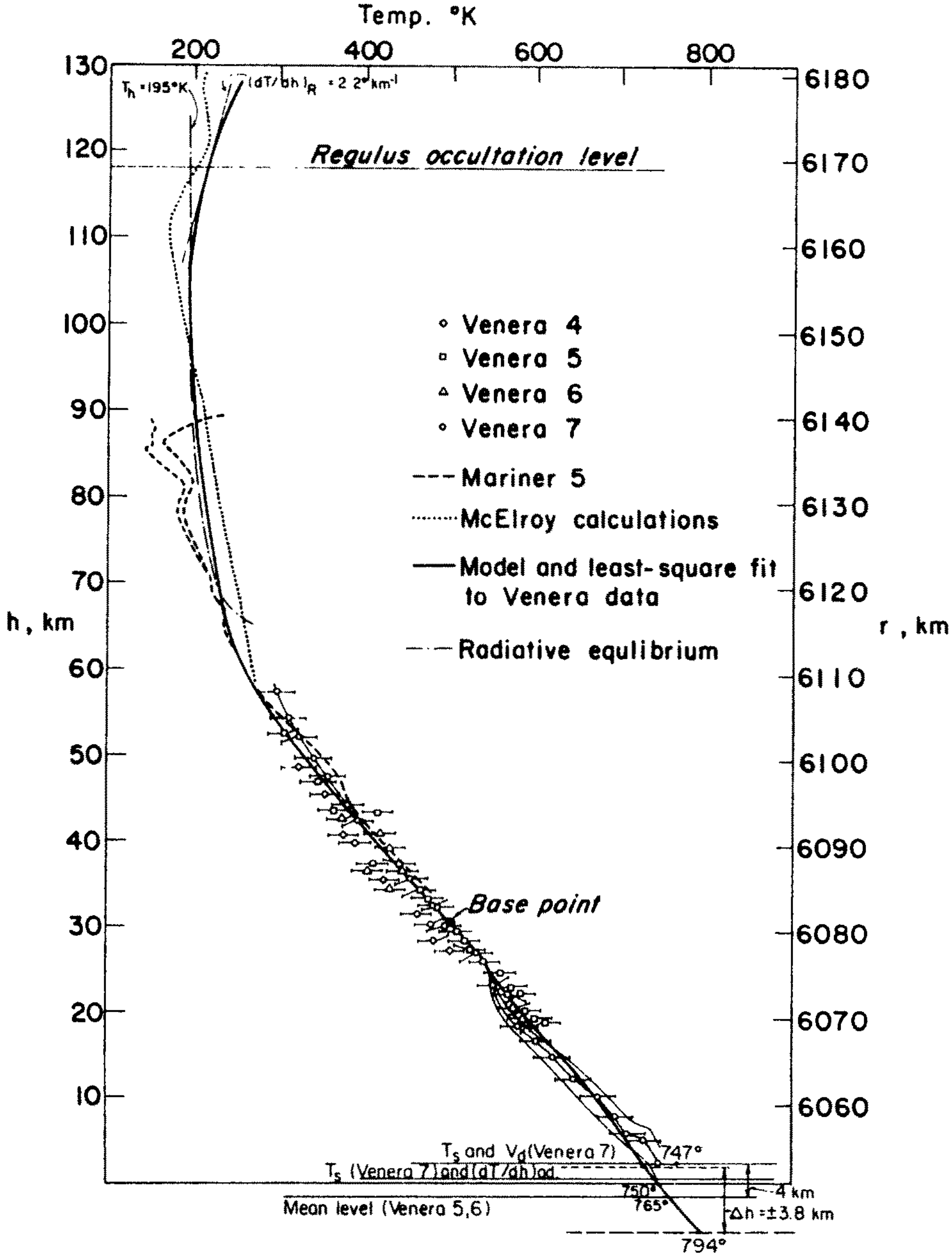

Fig. 1. Temperature profile of the Venus atmosphere as determined from the range of observations and theoretical calculations, after Marov (1972). Individual Venera temperature measurements are displayed.

surface of Venus is greater than that emitted from the surface of the earth by a factor $(740/290)^4 \simeq 42$. Thermal equilibrium at the surface therefore requires very large infrared opacity in the atmosphere and some mechanism for depositing heat at the surface.

Another important generalization about the Venus atmosphere is that it shows a remarkable degree of thermal mixing compared with the Earth. Manifestations of this thermal mixing include the almost adiabatic temperature profile vertically, and the smallness of temperature variations horizontally. An adiabatic region beginning at about 55–60 km altitude, and extending downward to a thin region of slightly subadiabatic lapse rates near 40–45 km altitude has been inferred from the Mariner radio occultation measurements. The Venera measurements suggest regions of slightly superadiabatic (by about 1%) lapse rates below 30 km altitude. However, these inferences require precise knowledge of the chemical composition of the atmosphere, so their reality is questionable. Latent heat effects on convection could perhaps explain the subadiabatic regions, but a sufficiently abundant condensate has not been found in the Venus atmosphere. A superadiabatic region in the free atmosphere is more difficult to explain; if real, it would be an entirely new phenomenon in atmospheric dynamics. The nearly adiabatic structure could be due to small-scale convection or planet-wide circulation. However, on earth the planet-wide circulations coupled with latent heat effects combine to produce a mean lapse rate that is only $\frac{2}{3}$ the adiabatic value.

Venus has an extensive, almost isothermal region from about 60 to 120 km altitude, analogous to the earth's stratosphere. It is in this region that the observable clouds lie, including the ultraviolet markings and thin haze layers observed by the Mariner 10 imaging system. The atmosphere is stably stratified at these levels and little vertical advection is to be expected. However, very strong horizontal winds or energetic wave motions are required to explain the observed 4-day rotation, and these motions are probably associated with horizontal temperature differences and radiative energy sources at these levels.

The exosphere of Venus appears to be as cold as that of Mars. Mariner 10 Lyman-alpha and helium airglow data are consistent with $T_\infty \simeq 400$ K (Broadfoot *et al.*, 1974; Kumar and Broadfoot, 1975), and a recent analysis of Mariner 5 Lyman-alpha data yields $T_\infty = 270$ K (Anderson, 1976). A comprehensive model of the composition, thermal structure, and circulation of the thermosphere (Dickinson and Ridley, 1975) shows that these temperatures cannot be understood in terms of mechanisms which reproduce the observed T_∞ on Mars (Stewart, 1972); fast vibrational quenching of CO_2 by O, or efficient downward eddy transport of heat, are possible solutions to the problem.

2.2. Horizontal thermal structure

In general, the smallness of the horizontal temperature differences on Venus reflects a very efficient planet-wide circulation. Microwave radiometric observations place an upper bound of about 20 K on the day–night temperature difference in the lower atmosphere and indicate a similar small equator–pole variation (Kellerman, 1965, 1966; Drake, 1962; Sinclair *et al.*, 1972). Preliminary temperature profiles determined by Veneras 9 and 10 differ by a few tens of degrees (Keldysh, 1976). Data on the region near the cloud tops consists of earth-based maps of the infrared brightness temperature in the 8–14 μm wavelength region (Murray, Wildey and Westphal, 1963) and observations by infrared radiometers on the spacecraft Mariner 10 (Chase *et al.*, 1974) and Veneras 9 and 10 (Avduevsky *et al.*, 1976; Keldysh, 1976). Interpretation of these data is greatly complicated by ambiguities introduced by uncertainties in the vertical and horizontal distribution of clouds, the clouds being the principal source of opacity at nearly all infrared wavelengths. Analyses of the earthbased observations by Ingersoll and Orton (1974) and preliminary results from Veneras 9 and 10 (Avduevsky *et al.*, 1976) indicate that the brightness temperature on the night side is 10°C hotter than that on the day side, with the poles about 25° hotter than the equator. However, the departures from a smooth limb darkening curve according to Mariner 10 45 μm observations correspond to thermal contrasts of only about 1 K at a level approximately 2 scale heights deeper in the atmosphere (Taylor, 1975). The difference between the temperature profiles recovered by the radio occultation experiments on Mariners 5 and 10 (Fjeldbo, Kliore and Eshleman, 1971; Howard *et al.*, 1974) are about 10 K at the same levels in the stratosphere of Venus. Part of the infrared variation is undoubtedly due to cloud height irregularities, although spatial and temporal thermal gradients probably contribute to some unknown degree.

At higher altitudes, above 90 km, the Venus circulation model of Dickinson and Ridley (1975) predicts temperature differences of more than 20 K between the sub-solar and anti-solar points. At still higher levels ($\sim$150 km above the surface), where heating by solar extreme UV dominates, the same model predicts day–night temperature differences of 300 K or more. These are larger by at least a factor of 2 than the values obtained from Mariner 10 UV spectrometer observations of the Venus exosphere (Broadfoot *et al.*, 1974).

Finally, Earth-based whole-disk spectra of Venus show brightness temperatures differing on the order of 20 K on different occasions (Hanel *et al.*, 1968; Gillett, Low and Stein, 1968). Since these measurements are beset by difficulties of accurate absolute radiometric calibration, some caution is necessary in interpreting these as true temporal variations.

2.3. Correlation of Thermal Structure with Other Features

Because of the extreme difficulty of spatially resolved Earth-based observations of even a relatively near-by planet like Venus, attempts to correlate the appearance, dynamical activity, and composition variables with thermal structure and with each other are so far inconclusive. Young (1975) has reported an attempt to correlate variations in the spectroscopic abundance of CO_2 with the rotational temperature and with the ultraviolet markings. No correlation was found. Barker (1975) looked for correlations between the apparent abundances of H_2O and CO_2 with a similar lack of success. Preliminary Venera 9 results show some features in both the IR and UV for some planetary scans which may show some correlations (Keldysh, 1976). It is inconceivable that phenomena such as the 4 day circulation could exist without an associated thermal structure providing driving forces for the strong winds. The apparent motion could also be a thermal wave, the UV markings produced by a still unidentified species condensing in the temperature minima and evaporating in the maxima. The highly irregular distribution of water vapor in space and time is likely to be associated with thermal structure, if only because of the importance of the water itself in cooling the atmosphere by radiation to space in its strong infrared absorption bands. Finally, the cloud morphology is likely to be strongly linked to the thermal structure. It is possible that the clouds maintain themselves at an almost constant temperature, moving up and down in altitude to adjust to variations in vertical temperature profile. Such an effect would account for the lack of thermal contrast observed in the Mariner 10 limb darkening scans, which would otherwise tend to contradict the predictions of radiative-dynamical models which require substantial contrasts to drive the motions. Systematic high-resolution vertical sounding measurements from a high-inclination orbiter of Venus coupled with direct measurements from entry probes at different locations on the planet are needed to provide data with the coverage, vertical discrimination and radiometric accuracy to resolve these questions.

3. Radiative Processes and the Thermal Structure

Sagan (1960) originally suggested that the high surface temperature of Venus might be caused by a greenhouse effect. In this mechanism, the atmosphere must have sufficient transmission at visible and near infrared wavelengths (shortward of about 3 μm) to allow a modest portion of the incident solar flux to penetrate to the surface of the planet. At the same time, it must have sufficient opacity at thermal infrared wavelengths to maintain the high surface temperature even in the face of the small solar flux expected to penetrate to low levels in the atmosphere. To be viable for Venus, such a model must also have sufficient horizontal motions to produce the observed relatively uniform horizontal temperature structure. While the greenhouse mechanism has now come to be regarded as more likely than competing dynamical mechanisms to account for the high surface temperature of Venus (Kalnay de Rivas, 1975), the fact remains that in the 15 years since its proposal we have accumulated precious little information on the deposition of solar energy and the thermal opacity of the Venusian atmosphere. We summarize the available information and uncertainties in these quantities below.

3.1. Deposition of solar energy

In a purely radiative-convective equilibrium model the thermal flux carried outward by the model will not be constant but will equal the net inward solar flux at each level. What is needed is therefore the profile of broad-band (0.3 to 3 μm) net (downward minus upward) solar flux at each level in the atmosphere.

The best data available are the preliminary solar radiometer data from Venera 9 and 10 (Avduevsky *et al.*, 1976) covering wavelengths from about 0.5 to

1.05 μm which includes some 17% of the solar energy absorbed by Venus. These recent data remain to be analyzed to yield a solar energy deposition profile.

The data most thoroughly analyzed to date are the Venera 8 photometer experiment measurements of the downward (only) flux from about 48 km to the surface in the wavelength interval between about 0.5 and 0.8 μm (Avduevsky *et al.*, 1973). An even smaller fraction ($\sim$10%) of the solar energy absorbed by Venus lies in this wavelength interval, however this range does include most of the solar energy which reaches the surface. Unfortunately, before the net flux can be obtained from these data, a scattering model consistent with the Venera 8 data and the albedo of the planet is needed to estimate the upward flux. As pointed out by Lacis and Hansen (1974) and Lacis (1975), a rather wide range of scattering models exists which can reproduce the Venera 8 data and the albedo of the planet. Lacis (1975) derived several possible cloud structures consistent with the data even under the restrictive assumption that the single scattering albedo of the cloud particles is independent of height. The results show that unless the ground albedo is very close to unity, the fraction of incident solar energy absorbed at the ground is in the range from 0.1 to 1% of the incident solar flux (corresponding to as much as 3% of the absorbed solar flux). Most of the absorbed solar energy is deposited in a broad region above 55 km altitude near the cloud tops. Because of the low density of this portion of the atmosphere, the heating rate also has a strong maximum near about 65 km altitude.

Nevertheless, the detailed vertical distribution of net solar flux remains quite uncertain. Pollack and Young (1975) attempted to explicitly add absorption by CO_2 and H_2O to one of Lacis's models and found a small but significant amount of energy to be deposited throughout the deep atmosphere. While the Venera 8 data already have been of great use in studies of the greenhouse mechanism (Pollack and Young, 1975), measurements of the profile of solar energy deposition are still needed. Upward as well as downward measurements having broad and flat spectral response and covering the altitude range from 80 km to the surface would be especially useful.

In the thermosphere, the rate of absorption of extreme ultraviolet (EUV) energy absorption must be reduced to allow for losses into chemical and airglow energy before the heating rate is obtained. The 'efficiency factor' for EUV heating used by Dickinson and Ridley (1975) was 0.3, but they indicate that it might be as low as 0.1. A lower EUV heating efficiency would tend to reduce the dayside exospheric temperature from the 600 K computed by Dickinson and Ridley to the observed value nearly 50% smaller. While other effects may be responsible for this difference, additional airglow observations by a UV spectrometer in Venus orbit would reduce the uncertainty in the EUV heating efficiency.

3.2. Thermal opacity

The contribution to the infrared opacity by a given gas species depends both on the wavelength location of its strong absorption bands and its abundance in the atmosphere. Because CO_2 is by far the most abundant gas in the Venus atmosphere and because it has a number of permitted transitions in the infrared spectral region, it makes a major contribution to the thermal opacity. However, in common with other molecules, it absorbs strongly only close to its major band centers and therefore has major 'window' regions. The most notable of these are the 3–4 μm region, the 6–9 μm region, and the region longward of 20 μm (Pollack, 1969).

Trace constituents may make an important contribution within the CO_2 window regions. Water vapour may play a major role in this regard since its strong absorption features nicely complement those of CO_2 in spectral location. However, the mixing ratio of water vapor is strongly limited within the region of the sulfuric acid clouds and thus it may be important only below these clouds. In fact, Veneras 9 and 10 seem to indicate a high H_2O/CO_2 mixing ratio (between 0.5 and 2×10^{-3}) below the clouds (Keldysh, 1976). Other trace gases such as SO_2 could also supply infrared opacity. To properly evaluate which gases make an important contribution to the infrared opacity, we must first know the composition of Venus' atmosphere as a function of altitude. In general, gases need to be present in concentrations in excess of 1 ppm if they are to be of importance for the infrared opacity. Also, of course they must have transitions in the window regions of CO_2. Thus for example, such inert gases as N_2 and Ar are not of interest for this question.

Cloud particles may also make an important contribution to the infrared opacity of the atmosphere (Knollenberg *et al.*, 1977). Their overall importance depends on the vertical extent of the clouds, the composition of the cloud particles and the particle size distribution function. Venera 8 results indicate the main cloud layer may have considerable vertical extent – from above 60 km to perhaps as low as 35 km. In this case, cloud particles may be a very important source of infrared opacity, though of course they will not be important in regions of the atmosphere having a low aerosol concentration. Cloud particles are a very useful source of infrared opacity since many plausible types of particles, including H_2SO_4, absorb strongly throughout most of the infrared spectral range. However, the strength of their absorption depends critically on the particle size distribution function. In general, it is only the larger particles, ones with radii in excess of about 1 μm, that have extinction cross-sections at thermal wavelengths comparable to their geometrical cross sections (Pollack and Young, 1975). Thus, to properly evaluate this type of opacity, we need to know the concentration of cloud particles as a function of altitude (or optical depth), their composition and their size. It is of course also very useful to measure 'directly' their contribution to the infrared opacity. The nephelometer and visible radiometer experiments aboard Veneras 9 and 10 should be of great use in determining the concentration of cloud particles at various altitudes (Marov *et al.*, 1976).

3.3. Current State of Radiation Calculations

As a result of new data obtained from spacecraft and Earth-based observations, it has been possible recently to test the greenhouse model in a more thorough fashion than had been possible previously, i.e., there has been a significant narrowing in the freedom with which one can choose the parameters of the greenhouse model. The important new data are the photometer observations carried out on the Venera 8 spacecraft (Avduevsky, 1973) and an identification of the composition of the visible cloud layer (Young, 1973; Sill, 1972; Pollack *et al.*, 1974). The former implied that the surface absorbs about 3% of the total solar energy absorbed by the planet (Pollack and Young, 1975). It also constrained the vertical profile for the deposition of solar energy, although it did not yield a unique profile (Lacis and Hansen, 1974). The latter result indicated that the visible cloud layer is composed of a water solution of concentrated sulfuric acid. As a result, the amount of water vapor and hence its contribution to the infrared opacity is severely limited within the region occupied by the sulfuric acid clouds. However, sulfuric acid is a very good absorber at most infrared wavelengths.

Pollack and Young (1975) constructed a greenhouse model for a horizontally averaged Venus, with model parameters consistent with the above constraints. They found it possible to reproduce approximately the high surface temperature. However in doing this they exercised the freedom which they still had in the values of certain variables. For example, they selected a mean particle radius of 3 μm at visible optical depths in excess of unity rather than a value of 1 μm which is known to apply at smaller optical depths. When a particle radius of 1 μm was used throughout the sulfuric acid clouds, assumed to extend to the 35 km altitude level, they were unable to obtain a high surface temperature. This was because the cloud aerosols were unable to supply enough infrared opacity. The computed surface temperature for their successful model was 650 K *vs.* the observed value of 750 K. However, further adjustments in the model parameters probably would have resulted in still better agreement. It is of some interest that the Venera 9 and 10 nephelometer experiments seem to indicate increasing particle size at lower altitudes (Marov, 1976).

The radiative calculations of Pollack and Young were also successful in obtaining a reasonable match to the observed vertical temperature profile. In these calculations the radiative equilibrium temperature gradient was adjusted to the adiabatic value when the former exceeded the latter. Pollack and Young found that their model atmosphere exhibited an adiabatic gradient at pressures in excess of 15 atm, i.e., at altitudes less than about 49 km.

Quite clearly the greenhouse model can be completely tested only when the relevant parameters of the Venus atmosphere are all well defined from empirical observations and there are no remaining degrees of freedom in the model parameters. Among the parameters of importance in this regard, which are most needed, are the atmospheric composition including its vertical profile, the composition, number density, and particle size of the clouds particles as a function of altitude, and the vertical profile of the solar energy deposition.

We should briefly mention that the most plausible alternative models to the greenhouse model for the high surface temperature are models where the planet's internal heat or atmospheric circulation play a major role in heating the surface. The former model seems unlikely at present since plausible values for the internal heat flux, based in part on terrestrial analogy, lie about two orders of magnitude below the amount of solar energy that reaches the surface according to the Venera 8 photometer experiment. The most recent and sophisticated calculations of the general circulation of the atmosphere imply that the density stratification of the atmosphere prevents the atmospheric dynamics from playing a major role in heating the surface (Kalnay de Rivas, 1975).

While the above discussion indicates that radiative calculations may provide useful insights into the cause of the high surface temperature and may be able to reproduce the vertical temperature structure, they are very deficient by themselves in accounting for the observed relatively small horizontal temperature contrasts. Thus, radiative calculations need to be incorporated within a general circulation model if we are to completely understand the thermal balance of the atmosphere of Venus.

4. Dynamical Processes and the Thermal Structure

Averaged over time and considered as a whole, Venus is in thermal balance with the Sun and space. At any one time it is more nearly in this balance than most planets because of its virtually uniform cloud cover, its nearly circular orbit and the small inclination of its spin axis to its orbital plane. In this respect it is an ideal planet for study because its thermal forcing is so steady. While the planet as a whole is in balance, different regions and zones are in radiative *imbalance*. The planet's low latitudes gain more heat from the sun than they lose to space and can be thought of as forming the 'boiler' of a planetary heat engine whose working substance is its atmosphere. High latitudes lose more heat to space than they absorb from the sun and form the 'condenser' of the engine. The radiative imbalance generates motions which redistribute heat over the planet.

4.1. Temperature contrasts between the equator and the poles

Assuming that the entire energy input into the atmosphere of Venus is due to absorption of solar energy somewhere in the atmosphere, the differences in the vertically integrated energy deposition are mainly due to the sphericity of the planet. If A is the local albedo (practically constant over the planet), S the solar constant at Venus and θ the solar zenith angle at longitude λ and latitude ϕ on the planet, then the energy absorbed in a unit area of atmosphere centered at (λ, ϕ) is $S(1-A)\cos\theta$. The average energy absorbed in the atmosphere over one solar day is thus $S(1-A)(\cos\phi)/\pi$ per unit area of atmosphere.

Whereas solar energy is absorbed in the sun-lit hemisphere only, energy is lost to space radiatively over the entire planet. Ground-based measurements indicate that the infrared energy loss by Venus decreases by about 10% between the equator and 45° latitude (Ingersoll and Orton, 1974). For the sake of argument one may treat the radiative loss as constant over the planet which amounts to a uniform brightness temperature, T_e, equal to about 240 K. The net loss or gain of energy from a region on Venus can thus be easily identified by comparison of $\sigma(T_e)^4$ with $(1-A)(\cos\phi)/\pi$. For a value of T_e of 240 K there is no net loss or gain of energy at a latitude of about 38° when the average is taken over one solar day.

The excess energy equatorward of this latitude must be transferred to the higher latitudes where there is a net energy deficit in order that global radiative equilibrium be maintained. There are presumably no oceans and thus unlike the terrestrial case where up to 40% of energy transfer is through oceans and the hydrologic cycle, the bulk of the energy transfer on Venus must be in the atmosphere. In view of the small pole–equator temperature contrast reported at the surface of the planet (Sinclair *et al.*, 1972) and at the top of the clouds (Murray, Wildey and Westphal, 1963; Ingersoll and Orton, 1974) the meridional energy transports in the atmosphere of Venus must be very efficient indeed. This energy transfer can take place on Venus in many ways – through transfer of internal energy, latent heat or even kinetic energy. In particular the transfer of energy to higher latitudes can take place by transport through a mean meridional circulation or by eddies or by a combination of the two. Whether the mean mode of energy transport or the eddy mode is dominant depends on the dynamics of atmospheric motions.

Analysis of Mariner 10 images indicate a comparatively steady meridional flow of about 10–15 m s^{-1} in the stratosphere. While this is an order of magnitude smaller than the zonal motions (Suomi, 1974) it is large compared to the terrestrial case for example. No data on meridional winds is available at altitudes below the cloud tops. On earth the poleward transports are predominantly due to eddy circulation rather than by a mean meridional circulation (Lorenz, 1967) and are thus very difficult to evaluate. On Venus, fortunately, there are indications that the reverse may be true. The eddy components of motions seem smaller than the mean motions as also evidenced by the symmetry and homogeneity of the UV features in Mariner 10 images. In the stratosphere near the cloud tops the 8–14 μm thermal maps indicate that the thermal field is also more nearly homogeneous than on earth and thus the mean meridional circulation may accomplish the bulk of the required energy transport.

Since there are indications that the vertical structure may vary with latitude on Venus, the ability of different machanisms to transfer energy, angular momentum and mass to higher latitudes is intimately related to the local vertical structure of the atmosphere and embedded smaller scale motions. In addition to accurate measurements of the meridional motions, careful targeting of multiple entry probes is needed to provide a good idea of the spatial variation of the vertical structure of the atmosphere which drives these motions.

4.2. Diurnal temperature contrasts

Despite the slow rotation of the planet, the day–night surface temperature differences observed are smaller than the accuracy of the measurements (Sinclair *et al.*, 1972; Kellerman, 1965, 1966), again implying efficient horizontal heat transport.

Stone (1975) has shown that throughout the atmosphere of Venus up to 80 km the radiative equilibrium temperature structure can be expected to be appreciably modified by the dynamical transports since the advective time scale for Venus is much shorter than the radiative relaxation time. Kuz'min and Marov (1975) also indicate that the departure from a state of geostrophy on Venus implies that the main contribution to heat transfer due to circulation should come from the nonlinear advective terms.

In the upper atmosphere, the day–night temperature differences should be larger. Dickinson and Ridley (1975) predict a flow from the warm subsolar point across the terminator, and a descending tongue of air at 10^{-2}–10^{-1} μ bar (heated by adiabatic effects) about 30° beyond the terminator. On the antisolar side of this tongue lies a cool stagnation cell. A measure of the extent of vertical turbulent mixing is needed to judge the modifications to this picture caused by that process.

To make progress in understanding the horizontal temperature variations in longitude and latitude in both the lower and upper atmosphere, measurements of temperature structure, wind, and net radiative heating are needed throughout the atmosphere at several locations on the planet in addition to the determination of the spatial structure of the thermal energy radiated to space by the planet.

4.3. Dynamics and the vertical temperature structure

While dynamical transport is clearly needed to account for the horizontal structure of the temperature field, the role played by vertical dynamical transport in establishing and maintaining the vertical temperature structure is less certain at present. Venera 7 and 8 data have been used to infer the existence of appreciable vertical motions (as much as 5 m s^{-1}) in the lower atmosphere of the planet (Ainsworth and Herman, 1975). Indeed for some assumptions of atmospheric composition, the Venera 8 temperature profile appears appreciably convectively unstable almost up to 40 km above the surface (Limaye and Suomi, 1976). Nevertheless the model calculations of Kalnay de Rivas (1975) indicate that without a strong greenhouse effect, dynamical circulation downward resulting from the deposition of solar energy high in the atmosphere does not extend to sufficiently deep levels to produce the observed high surface temperatures by adiabatic compression.

The reader is referred to the paper in this volume by Schubert *et al.* (1977) for a more complete discussion of the possible modes of dynamical heat transport, and to the paper by Knollenberg *et al.* (1977) for a discussion of the possible role of latent and chemical heats of formation of various cloud constituents on the thermal structure. About all that is certain at present is the complexity of the nonlinear interactions between the thermal structure which drives the dynamical transport of heat which in turn affects the distribution and optical properties of the cloud particles and modifies the thermal structure. Before one can begin to understand the thermal balance of the planet, the factors affecting that balance such as the circulation pattern of the atmosphere, the thermal emission of different regions of the planet, the solar energy deposition profile, the sources of thermal opacity, and the temperature structure itself all need to be known much better than they are at present.

5. Expected Contributions of Pioneer Venus

As described elsewhere in this volume (Colin and Hall, 1977), the Pioneer Venus Orbiter and Multiprobe missions to Venus are planned to arrive at Venus in December of 1978. Aboard the orbiter, probe bus and four entry probes will be a number of instruments planned to make observations of many of the quantities identified above as critical in understanding the thermal balance of the atmosphere of the planet. In this section we review in turn our needs in each of these areas and attempt to evaluate the contribution which the Pioneer Venus mission can make to each.

5.1. Temperature structure

It is obvious that a detailed knowledge of the distribution of heat in the atmosphere of the planet is essential to understanding the processes that maintain that distribution. We very much need accurate temperature–pressure profiles throughout the atmosphere at many locations on the planet well separated in longitude and latitude. Temperature differences referred to constant pressure levels will be especially useful in understanding the dynamical drives of the atmosphere and the structure and evolution of the clouds.

The Pioneer Venus experiments are expected to establish the temperature structure of the atmosphere below the clouds with precision at four entry sites generally well separated in longitude and latitude. They will also extend the measurements of thermal structure upwards from the present limit of 75 km to about 200 km. Several experiments will contribute to this extended definition. The Comparative Atmosphere Structure experiment (LAS/SAS), carried on the four entry probes, will measure the temperature and pressure below the clouds on both the day-side and night-side of the planet to an accuracy goal of $\frac{1}{4}$ K and 0.5% of pressure. It will also determine the absolute altitude of the measurements, with an accuracy goal of 100 to 200 m. The lower atmosphere temperature structure down to about 37 km also will be determined by the radio occultation technique from the orbiter.

Above 65 km, temperature profiles will be determined to an accuracy of better than one degree and a few percent of pressure by several contributing experiments, both *in situ* and remote sensing. The *in situ* measurements include accelerometry (LAS/SAS), radio tracking of the orbiter (OAD), and density scale height measurements from the Neutral Mass Spectrometers aboard both the bus (BNMS) and orbiter (ONMS). The remote sensing includes vertical temperature sounding by the Infrared Radiometer (OIR), and ultraviolet emission measurements by the Ultraviolet Spectrometer (OUVS), both aboard the orbiter. These experiments will be complementary, in that the *in situ* measurements can serve as 'ground-truth' for the remote sensing, while the remote measurements from the orbiter will give extensive global coverage. Detailed descriptions of these instruments appear elsewhere in this volume (Colin and Hunten, 1977). Table I summarizes the expected contributions of the Pioneer instruments to understanding the thermal balance of the planet.

5.2. Deposition of Solar Energy

The deposition of solar energy forms the input to the planetary greenhouse and by heating the atmosphere also produces a basic drive for the dynamical redistribution of heat over the planet. The profile of broadband (0.3 to 3 μm) net flux with altitude is needed from altitudes greater than 80 km to the surface at several solar zenith angles.

From about 65 km altitude to the surface the Solar Flux Radiometer (LSFR) aboard the large probe and the Net Flux Radiometer (SNFR) aboard the small probe that is targeted to descend in daylight will measure this quantity. The LSFR yields both the upward and downward fluxes from about 0.4 to 1.8 μm to an accuracy goal of 1% at a vertical resolution varying from about 700 to 100 m. Further, solar deposition outside the passband of the LSFR can be computed from the size distribution and optical properties of the cloud particles. The Cloud Particle Size Spectrometer (LCPS) and Nephelometer (LN) aboard the large probe will measure the size distribution and volume scattering cross-section of the cloud particles throughout the atmosphere. In addition, a narrower spectral channel of the LSFR measures the diffuse scattering and transmission characteristics of each layer of the atmosphere which can be inverted to yield the variation with altitude of the single scattering albedo of the cloud particles and the optical depth of the clouds.

On the small probes, the SNFR measures the net flux over a very broad spectral band that includes both the solar and the thermal radiation field. This quantity together with the measurements of the thermal net flux alone by the Infrared Radiometer (LIR) aboard the large probe and by the SNFR instruments aboard the two small probes landing on the dark side of the planet may also yield an independent determination of the solar deposition profile at a second location on the planet. The three small probes also each contain Nephelometers (SN) which will indicate the variations in cloud properties at these locations on the planet.

Remote sensing methods can be used to obtain the solar deposition in the portion of the atmosphere above that accessible to the probes. The Cloud

TABLE I

Pioneer measurements related to the thermal balance of the atmosphere of venus

Atmospheric property	Experiment	Quantities measured	Vertical range of measurement	Vertical resolution	Spatial coverage	Accuracy
Temperature structure	Comparative Atmospheric Structure (LAS/SAS)	Temperature Pressure Altitude	67 km to surface 67 km to surface 67 km to surface	Few 100 m	On each of 4 probes	1/4 K 1/2% 100–200 m
		Temperature Pressure Altitude	200 km to 67 km 200 km to 67 km 200 km to 67 km	Few 100 m	On each of 4 probes	5 K 3% 300 m
	Orbital Infrared Radiometer (OIR)	Emitted intensity in 7 narrow spectral channels	10^{-9} mb to 250 mb pressure ($\sim$160 to 60 km)	5–10 km	3 km resolution	<0.5 K
	Ultraviolet Spectrometer (OUVS)	UV limb profiles from 1216 to 2890 Å	0 to 10^{-3} μb	3 km	120 km resolution	$\sim$10%
	Retarding Potential Analyzer (ORPA)	Ion temperature	0 to 10^{-4} μb	Variable	Few km resolution	$<5\%$
	Electron Temperature Probe (OETP)	Electron temperature	0 to 10^{-4} μb	Variable	Few km resolution	$<5\%$
Solar energy deposition	Solar Flux Radiometer (LSFR)	Intensity from 0.4–1.8 μm at 5 zenith angles	67 km to surface	700–100 m	On large probe	1% in upward and downward solar flux
	Net Flux Radiometer (SNFR)	Net flux in 0.3–30 μm interval	70 km to surface	Few 100 m	On one small probe on the day-side	Depends on substraction of net IR flux
	Cloud Photopolarimeter (OCPP)	Intensity and polarization at various scattering geometries	Above about 65 km	Few km	15–30 km resolution for imaging; few hundred km resolution for polarization	Net flux computed from models to few %

	Orbital Infrared Radiometer (OIR)	Local and global bond albedo	—	—	3 km resolution (local albedo)	Few %
Thermal radiative flux	Large Probe Infrared Radiometer (LIR)	Difference between up and down intensity from 3–50 μm	67 km to surface	Few 100 m	On large probe	Net flux to ± 0.25 W m^{-2}
	Net Flux Radiometer (SNFR)	Net flux from 0.3–30 μm	67 km to surface	Few 100 m	On 2 small probes in darkness	Net flux to few %
	Orbital Infrared Radiometer (OIR)	Emitted flux from 8 spectral channels between 0.2–55 μm	160 km to 60 km	7 levels at pressure <250 mb	1000 points per orbit	1%
Radiative opacity	Large Probe Neutral Mass Spectrometer (LNMS)	Atmospheric composition	67 km to surface	60 mass spectra during descent	On large probe	1 ppm resolution from 1–208 AMU, 20% accuracy
	Large Probe Gas Chromatograph (LGC)	Abundance of heavier gases	67 km to surface	56–142 m	On large probe	8–54 ppm resolution
	Large Probe Infrared Radiometer (LIR)	Net flux in 2H_2O lines and between CO_2 lines for cloud opacity	67 km to surface	Few 100 m	On large probe	Sensitive to H_2O/CO_2 between 0.3 and 500 ppm
	Orbital Infrared Radiometer (OIR)	45–55 μm water vapor opacity	110–70 km	5 km	3 km resolution	A few precipitable μm resolution
	Cloud Particle Spectrometer (LCPS)	Cloud particle size, concentration, and aspect ratio	68 km to surface	800–100 m	On large probe	Varies from 0.5 to 50 μm over 4 size ranges for particles from 0.5 to 500 μm
	Nephelometer (LN/SN)	Back-scattering cross section/volume	68 km to surface	100–10 m	On each of 4 probes	10 μm^2 cm^{-3}

TABLE I (*continued*)

Atmospheric property	Experiment	Quantities measured	Vertical range of measurement	Vertical resolution	Spatial coverage	Accuracy
Radiative opacity (*cont.*)		Ambient light level in uv and visible	68 km to surface	100–10 m	On each of 4 probes	1% of each of 2 ranges from 10^{-5} to $10^{-1}\ \mathrm{W\,m^{-2}\,sr^{-1}\,Å^{-1}}$
	Cloud Photo-polarimeter (OCPP)	Cloud particle size distribution	Above 65 km	Few km	Few 100 km	Few %
		Refractive index from model fits to polarization data	Above 65 km	Few km	Few 100 km	Better than 1%
Total flux divergence	Net Flux Radiometer (SNFR)	Net flux from 0.3–30 μm	67 km to surface	Few 100 m	On each of 3 small probes	Few %
	Large probe infrared and solar flux radiometer (LIR & LSFR)	Thermal and solar net fluxes separately	67 km to surface	Few 100 m	On large probe	10%
Wind field	Radio Science (DLBI)	Double long baseline interferometry	80 km to surface	Few km	On each of 4 probes	Few tenths of $\mathrm{m\,s^{-1}}$
	Comparative Atmospheric Structure (LAS/SAS)	Vertical wind from acceleration history and aerodynamic properties	67 km to surface	Few 100 m	On each of 4 probes	$\sim 0.1\ \mathrm{m\,s^{-1}}$
	Cloud Photo-polarimeter (OCPP)	UV imaging	Above about 65 km	Few km	15–30 km resolution	Few $\mathrm{m\ s^{-1}}$

Photopolarimeter/Imager (OCPP) aboard the orbiter will determine the cloud particle refractive index, shape, and size distribution, the pressure at the cloud top and the vertical distribution of cloud and haze particles within and above the visible top of the clouds (Hansen and Hovenier, 1974). From this data the cloud phase function and optical thickness distribution can be derived. Together with the intensity measurements made by the OCPP and the broad-band albedo measurements of the Infrared Radiometer (OIR) aboard the orbiter, the solar deposition can be computed down to the level where the probes begin making direct measurements.

In the thermosphere, the Infrared Radiometer (OIR) will measure the (non-LTE) emissions in the 15 μm band of CO_2 up to an altitude of 160 km, somewhat above the maximum solar EUV heating region. The ultraviolet spectrometer (OUVS) will measure the rate of photoionization, and hence heat deposition, by observing the intensity of emissions from carbon dioxide ions excited during the photoionization process.

The complementary probe and orbiter measurements should greatly extend our knowledge of the profile of solar deposition. Perhaps the greatest limitation of the Pioneer determination of this quantity is the fact that for the lower atmosphere, it can be obtained at essentially only a single solar zenith angle of about 70° because of constraints imposed by the communication system. The larger energy deposition at smaller solar zenith angles will have to be modeled.

In addition to the net solar flux and the temperature structure, confirmation of the greenhouse theory requires comparison of the measured net solar flux with the net thermal flux. The thermal flux can be obtained either from a direct measurement or from a determination of the sources of thermal opacity followed by computation of the thermal radiative flux from the temperature structure. The direct determination of a substantial average downward dynamical heat transport in the atmosphere would also be inconsistent with greenhouse explanations of the high surface temperature. Experiments aboard the Pioneer Venus missions will obtain measurements of all three quantities – the thermal radiation field, the sources of opacity, and the vertical winds.

5.3. Thermal radiative flux

The broadband channel of the Infrared Radiometer (LIR) aboard the large probe is sensitive to thermal radiation between 3 and 50 μm wavelength at two viewing angles located 45° above and below the local probe horizon. The signed difference between the downward and upward intensities, proportional to the net flux, is telemetered every 6 s giving a vertical resolution of 250 m or better. The wavelength response of this instrument will measure 90% of the thermal radiation from parachute deployment at 67 km altitude to the surface.

In addition, the SNFR instruments aboard the two small probes entering the atmosphere on the night side will measure the net broadband radiative flux between 0.3 and 30 μm from about 70 km altitude to the surface at two other locations on the planet.

At higher altitudes, the infrared radiometer aboard the orbiter (OIR) will map the thermal emission from the planet in seven narrow spectral channels in absorption bands of various strengths which probe altitudes between 60 and 160 km (see Taylor, 1974; Houghton and Taylor, 1975, and Table I). Further, the Pioneer instruments will measure the thermal emission of very high levels in the atmosphere ($P \leq 10^{-4}$ mb) where local thermodynamic equilibrium (LTE) is expected to break down. Under these conditions, the rate at which the atmosphere cools to space depends on poorly understood processes of radiative exchange between molecules. Direct measurements of the thermal emission from these levels from Pioneer offer the first opportunity to study these effects by comparing the observed intensities to models of the radiative transfer mechanisms which dominate under the appropriate conditions (e.g., Dickinson and Ridley, 1975). Also, the measured effective radiating temperature can be compared to the actual kinetic temperature inferred from measurements of the CO_2 scale height by the Neutral Mass Spectrometer (ONMS), and from the airglow scale heights observed by the Ultraviolet Spectrometer (OUVS). Further information on the thermal state of the upper atmosphere will come from measurements of the ion and electron temperatures by the Orbiter's Langmuir Probe (OETP) and Retarding-Potential Analyzer (ORPA).

5.4. Thermal opacity

While the operation of a greenhouse mechanism can be inferred from measurements of the solar and thermal fluxes, an understanding of the mechanism requires a knowledge of the sources of thermal opacity as indicated in Section 3. Perhaps our greatest needs in this regard are measurements of the mixing ratio of water vapor throughout the atmosphere and a knowledge of the thermal opacity of the cloud particles which depends on their size, composition and number density.

The LIR instrument aboard the large Pioneer Venus probe helps determine the opacity from both of these sources below 67 km altitude by including measurements at narrow spectral channels from 6 to 7 μm, 7 to 8 μm and 8 to 9 μm in addition to its broadband channel. These spectral regions, which lie near the maximum of the blackbody curve for the temperature range which will be encountered, should be relatively transparent in a pure carbon dioxide atmosphere. The first two channels, however, will be strongly affected if water vapor is present in the atmosphere, and their relative signal intensity will permit inference of the water vapor opacity at wavelengths other than those measured. The third, or 8 to 9 μm channel, will determine the opacity of the clouds as the probe descends to the surface, since this wavelength is free of known gaseous absorption. In addition, the Neutral Mass Spectrometer (LNMS) and Gas Chromatograph (LGC) aboard the large probe will be sensitive to very small mixing ratios of other atmospheric constituents in addition to water vapor which can contribute thermal opacity.

Also, the LCPS will measure the size distribution of the cloud particles from 67 km altitude to the surface. Together with an assumed composition, this allows computation of the cloud opacity. The computed opacity msut agree with that determined from the LIR 8 to 9 μm spectral channel. The nephelometers aboard all four probes (LN/SN) give an indication of the differences in vertical distribution of the clouds at different locations on the planet.

In the region above the main cloud top ($P \leq 1$ atm) the OIR narrow spectral channel at 50 μm will indicate the global distribution and variability of water vapor. The vertical and horizontal distribution of cloud opacity can be obtained from the OIR narrow band measurements at various viewing geometries, and compared with the cloud characteristics determined by the Cloud Photopolarimeter/Imager (OCPP) also aboard the orbiter.

5.5. Total flux divergence

In addition to the solar and thermal radiation field and the sources of opacity, we very much need to evaluate and understand the dynamical transport of heat occurring in the atmosphere of Venus. As mentioned earlier, the drive for the dynamical transport is the difference in the total (solar and thermal) net radiative flux at different levels of the atmosphere. Aboard the Pioneer Venus large probe, the solar and thermal radiative flux divergences are measured separately by the LSFR and the LIR instruments. Aboard each of the three small probes, the total net flux is measured by the SNFR. The LIR and the SNFR measure the net flux directly and operate so as to compensate for unwanted bias errors.

Especially important is the fact that measurements of the total flux divergence will be obtained at several locations on the planet simultaneously. Observations will be obtained at both high and low latitudes at about the same longitude, and on the day and night sides at about the same latitude. These data will greatly help in understanding the energy transported by the wind field.

5.6. Wind field

A measurement of the wind field in addition to the temperature structure gives the thermal energy transported by dynamical processes. The winds in the stratosphere can be obtained globally from the UV images obtained by the OCPP aboard the Pioneer Venus orbiter in a manner similar to that used in the study of the Mariner 10 images (Suomi, 1974). The Pioneer data will be more complete because the orbiter will yield data for a full solar day at Venus. In addition, the OCPP operating in the photopolarimetry mode will determine the characteristics of the cloud particles in the UV bright and dark areas and their vertical distribution as an aid in separating wave and particle motions.

Below the levels accessible to the OCPP, the radio science experiments (MWIN, MPRO) will measure the wind field at the entry sites of each of the four probes by using the Doppler shifts, coupled with interferometry along two long baselines (DLBI) of the radio signals of each probe compared with the probe bus. The vector velocity of each of the probes relative to the center of the planet can be obtained in this way. The horizontal velocity components are influenced by the winds, and horizontal wind speeds of a few tenths of a meter per second can be measured with a vertical resolution of the order of a few kilometers (Colin and Hunten, 1977). The determination of the vertical winds from the radio data requires in addition a knowledge of the aerodynamics of the probe descent and may be somewhat less accurate.

Further, the CAS experiment (LAS/SAS) which includes measurements of temperature, pressure, and acceleration can yield the vertical component of the wind at each probe entry site from the acceleration history of the probe and a knowledge of its aerodynamic properties. Vertical wind velocities can be obtained to an accuracy of about 0.1 m s^{-1} by this method for a probe exhibiting a steady drag coefficient (Schubert *et al.*, 1977).

Particularly significant is the fact that several probes will enter the atmosphere in widely separated regions. All three components of the wind field in the lower atmosphere will be determined at a high latitude where the flow in the stratosphere seems to be at nearly constant angular velocity (Suomi, 1974), and also at lower latitudes where stratospheric flow seems quite different. Also, probes will enter on both the day and the night sides of the planet at similar latitudes.

In summary, the Pioneer Venus instruments will map the global temperature structure, solar and thermal radiation fields, and the optical properties and motions of the clouds in the region above about 60 km altitude at high spatial resolution over an entire rotation of the planet. The probes will measure the vertical variations in the same basic quantities at four different locations on the planet from about 65 km altitude to the surface. The large probe in addition will determine the abundance of minor atmospheric constituents and obtain crucial information on the sources of thermal opacity in the atmosphere of Venus. The Pioneer Venus mission will thus provide much of the data essential to understanding the complex interplay between radiative and dynamical transport which controls the distribution of heat in the atmosphere of that planet, and also in our own.

References

Ainsworth, J. E. and Herman, J. R.: 1975, *J. Geophys. Res.* **80,** 173.

Anderson, D. E. Jr.: 1976, *J. Geophys. Res.* (in press).

Avduevsky, V. S., Marov, M. Ya., Moshkin, B. E., and Ekonomov, A. P.: 1973, *J. Atmos. Sci.* **30,** 1215.

Avduevsky, V. S., Marov, M. Ya., Moshkin, B. E., and Ekonomov, A. P.: 1976, Paper presented at the COSPAR meeting held June 14–19 at Philadelphia, Pa.

Avduevsky, V. S., Ishevsky, V., and Marov, M. Ya.,: 1976, Pravda No. 52 (2102), NASA TT F-16934.
Barker, E. S.: 1975, *Icarus* **25,** 268.
Berge, G. L., Muhleman, D. O., and Orton, G. S.: 1972, *Icarus* **17,** 675.
Broadfoot, A. L., Kumar, S., Belton, M. J. S., and McElroy, M. B.: 1974, *Science* **183,** 1315.
Chase, S. C., Miner, E. D., Morrison, D., Münch, G., and Neugebauer, G.: 1974, *Science* **183,** 1291.
Colin, L. and Hall, C. F.: 1977, *Space Sci. Rev.* **20,** 283
Colin, L. and Hunten D. M.: 1977, this issue, p. 451.
de Vaucouleurs, G. and Manzel, D. H.: 1960, *Nature* **188,** 28.
Dickinson, R. E. and Ridley, E. C.: 1975, *J. Atmos. Sci.* **32,** 1219.
Drake, F. D.: 1962, *Nature* **195,** 894.
Fjeldbo, G., Kliore, A. J., and Eshelman, V. R.: 1971, *Astron. J.* **76,** 123.
Fjeldbo, G., Seidel, B., and Sweetnam, D.: 1975, *J. Atmos. Sci.* **32,** 1232.
Gillett, F. C., Low, F. J., and Stein, W. A.: 1968, *J. Atmos. Sci.* **25,** 594.
Hanel, R., Forman, M., Stambagh, G., and Meilleur, T.: 1968, *J. Atmos. Sci.* **25,** 586.
Hansen, J. E. and Hovenier, J. W.: 1974, *J. Atmos. Sci.* **31,** 1137.
Houghton, J. T. and Taylor, F. W.: 1975, *J. Atmos. Sci.* **32,** 620.
Howard, H. T., Tyler, G. L., Fjeldbo, G., Kliore, A. J., Levy, G. S., Brunn, D. L., Dickinson, R., Edelson, R. E., Martin, W. L., Postal, R. B., Seidel, B., Sesplankis, T. T., Shirley, D. L., Stelzried, C. T., Sweetnam, D. N., Zygielbaum, A. I., Esposito, P. B., Anderson, J. D., Shapiro, I. I., and Reasenberg, R. D.: 1974, *Science* **183,** 1297.
Hunten, D. M. and McElroy, M. B.: 1968, *J. Geophys. Rev.* **73,** 4446.
Ingersoll, A. P. and Orton, G. S.: 1974, *Icarus* **21,** 121.
Kalnay de Rivas, E.: 1975, *J. Atmos. Sci.* **32,** 1017.
Keldysh, M. V.: 1976, Paper presented at the COSPAR meeting held June 14–19 at Philadelphia, Pa.
Kellerman, K. I.: 1965, *Radio Sci.* **90,** 1574.
Kellerman, K. I.: 1966, *Icarus* **5,** 478.
Knollenberg, R. G., Hansen, J. E., Ragent, B., Martonchik, J., and Tomasko, M. G.: 1977, *Space Sci. Rev.* **20,** 329.
Kumar, S. and Broadfoot, A. L.: 1975, *Geophys Res. Lett.* **2,** 357.
Kuz'min, A. D. and Marov, M. Y.: 1975, *Physics of the Planet Venus,* NASA Technical Translation TT F-16, 226.
Lacis, A. A.: 1975, *J. Atmos. Sci.* **32,** 1107.
Lacis, A. A. and Hansen, J. E.: 1974, *Science* **184,** 979.
Limaye, S. S. and Suomi, V. E.: 1976, (in preparation).
Lorenz, E. N.: 1967, *The Nature and Theory of the General Circulation of the Atmosphere,* World Meteorological Organization, Geneva.
Marov, M. Ya.: 1972, *Icarus* **16,** 415.
Marov, M. Ya., Avduevski, V. S., Borodin, N. F., Ekonomov, A. P., Kerzhankovich, V. V., Lysov, V. P., Moshkin, B. Ye., Rozhdestvensky, M. K., and Ryabov, O. L.: 1973, *Icarus* **20,** 407.
Marov, M. Ya., Lebedev, V. N., Lystsev, V. E. Kuznetsov, I. S., and Popanopulo, G. K.: 1976, paper presented at the COSPAR meeting held June 14–19 at Philadelphia, Pa.
McElroy, M. B: 1968, *J. Geophys. Res.* **73,** 1513.
Murray, B. C., Wildey, R. L., and Westphal, J. A.: 1963, *J. Geophys. Res.* **68,** 4813.
Pollack, J. B.: 1969, *Icarus* **10,** 314.
Pollack, J. B., Erickson, E. F., Witteborn, F. C., Chackerian, C., Jr., Summers, A. L., Van Kamp, W., Baldwin, B. J., Augason, G. C., and Caroff, L. J.: 1974, *Icarus* **23,** 8.
Pollack, J. B. and Young, R.: 1975, *J. Atmos. Sci.* **32,** 1025.
Rumsey, H. C., Morris, G. A., Green, R. R., and Goldstein, R. M.: 1974, *Icarus* **23,** 1.
Sagan, C.: 1960, *Astron. J.* **65,** 352.
Schubert, G., Counselman, III, C. C., Hansen, J., Limaye, S. S., Pettengill, G., Seiff, A., Shapiro, I. I., Suomi, V. E., Taylor, F. W., Travis, L., Woo, R., and Young, R. E.: 1977, this issue, p. 357.
Still, G. T.: 1972, *Comm. Lunar & Planet. Lab.* **9,** 191.
Sinclair, A. C. E., Basart, J. P., Buhl, D., and Gale, W. A.: 1972, *Astophys. J.* **175,** 555.

Stewart, A. I.: 1972, *J. Geophys. Res.* **77,** 54.
Stone, P.: 1975, *J. Atmos. Sci.* **32,** 1005.
Suomi, V. E.: 1974, Presented at Conference on the Atmosphere of Venus, Goddard Institute for Space Studies, New York, October 15–17.
Taylor, F. W.: 1974, *Appl. Opt.* **13,** 1559.
Taylor, F. W.: 1975, *J. Atmos. Sci.* **32,** 1101.
Westphal, J. A., Wildey, R. L., and Murray, B. C.: 1965, *Astrophys. J.* **142,** 799.
Young, A. T.: 1973, *Icarus* **18,** 564.
Young, A. T.: 1975, *J. Atmos. Sci.* **32,** 1125.